

EVALUATION OF ANGULAR DISTRIBUTION OF RADIATION DOSES TO UPGRADE RF-GUN TEST FACILITY IN SPRING-8

Nobuteru Nariyama, JASRI/SPring-8, Japan

Abstract

The allowable electron energies of the linac in the RF-gun test facility were increased from 30 MeV to 100 MeV in the past few years. The beamline branches near the bottom, and the branched beamline is angled at 30° to the side wall. As the background data for radiation safety, photon and neutron dose equivalent distributions around the lead and iron cylindrical targets struck by electrons were calculated with a Monte Carlo code as a function of the emission angle. The photon dose distributions outside the concrete shield around the loss points in the test facility were calculated using the targets and code, which showed the adequacy of the concrete shield wall and the effect of the local shield set before the loss point.

INTRODUCTION

In SPring-8, the allowable electron acceleration energy of the compact linac for the RF-gun test has been upgraded step-by-step. The first energy was 30 MeV, and it was increased to 65 MeV and then to 85 MeV in 2013. In 2015, an application for up to 100 MeV was filed with the authority.

The facility is located next to the 1-GeV linac, separated by 290-cm-thick concrete, as shown in Fig. 1 [1]. The electrons emitted from the photocathode RF gun are accelerated to the final energy before the chicane situated 6 m from the gun and incident on one of the dumps indicated as S1 and S2 in Fig. 1 either after travelling straight or after deflection by 30° , respectively. The total length of the linac will extend to 10 m after increasing the energy. The beam dumps are composed of graphite blocks backed by iron blocks with thicknesses of 50 cm and 10 cm in the longitudinal and lateral directions, respectively. Slits are located at S3 on the chicane and at S5 before the dump. 5-cm-thick lead blocks are fixed between the S5 slit and 140-cm-thick side wall. The area outside the concrete on the right side is the open air and uncontrolled area.

Thus, the arrangement was simple. However, the electrons travel diagonally toward the side wall in the compact room; hence, the emission intensity of radiation from the loss points at angles beside 0° and 90° was important. The angular distribution of photons has been found to depend on the target geometry [2]. In this study, the angular distribution of photon and neutron doses at electron injection energies of 30, 65, and 100 MeV were calculated with a Monte Carlo transport code and compared with analytical expressions to investigate the target size dependence. After confirming the validity of the inputs and determining suitable target sizes, the dose outside the shielding wall near the loss points was evaluated with the code.

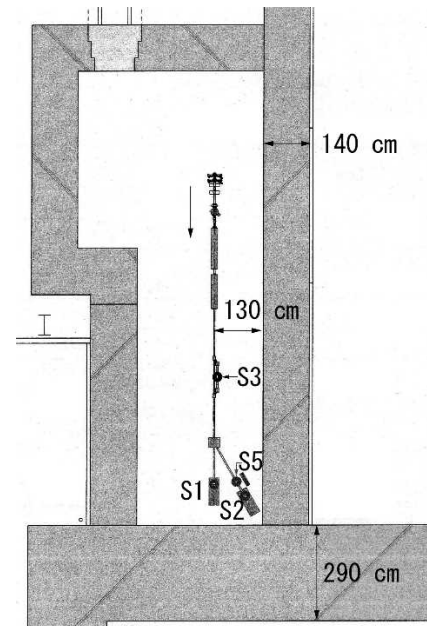


Figure 1: Layout of the RF-gun test facility. The shaded parts are ordinary concrete. S1 and S2 are the dumps, and S3 and S5 are the slits. S3 is on the chicane. Lead blocks are set near S5. The area outside the concrete on the right side is open air and an uncontrolled area.

CALCULATIONS

For the Monte Carlo calculations, the FLUKA code (Ver. 2011.2c.0) [3] was used with the Flair interface (ver.2.0-8) on 64-bit Fedora 21. A multicore CPU was used by assigning different random number seeds on each run. Electrons impinged upon the cylindrical target made of lead and iron, and the photon and neutron dose equivalents were scored at 1 m from the target as a function of the angle. The electron energies were 30, 65, and 100 MeV.

The target sizes for photon doses are important for the evaluation [2]. From the reported result [4] and our survey calculations, two sizes were used, depending on the emission angle as shown in Table 1. In the forward direction, a length of $2X_0$ and a radius of $3X_M$ were used, in which X_0 was the radiation length and X_M was the Moliere radius. In the backward direction, $10X_0$ and X_M were used for the length and radius. The limits of the forward and backward directions were set to 60° and 30° for lead and iron, respectively. The radiation lengths are 0.51 and 1.6 cm, and the Moliere radii are 1.1 and 1.3 cm for lead and iron, respectively.

Table 1: Cylindrical target sizes for photon doses. X_0 is the radiation length, and X_M is the Moliere radius.

Target	Angle	Length	Radius
Lead	0° - 60°	$2X_0$	$3X_M$
Lead	90° - 150°	$10X_0$	X_M
Iron	0° - 30°	$2X_0$	$3X_M$
Iron	45° - 150°	$10X_0$	X_M

The scoring mesh sizes were 4 cm in length and in radius in cylindrical coordinates. At 0°, a scoring radius of 1 cm was used because of the high gradient.

For neutrons, a large dependence on the target size was not observed in our calculations. Thus, $10X_0$ was used as the length, and $3X_M$ and X_M were used as the radius for lead and iron, respectively.

For the shielding calculations, the photon dose equivalents were calculated at an accelerating energy of 100 MeV, assuming 100% electron losses at the S3 and S5 slits. A lead target sized for the forward direction was used as the slits. Nine million histories were generated in the execution. The neutron doses outside the wall were found to be much lower than the photon doses.

RESULTS

Figures 2 and 3 show the photon ambient dose equivalent as a function of emission angle from the lead and iron targets, respectively. The statistical fluctuations were less than a few percent. Except at 0°, the distribution was almost the same independent of the energy while the doses at 30 MeV were smaller than the others in the forward direction. At 0°, the doses were less than $300E$, where E is the electron energy [2], while the magnitudes depended on the integrated sizes of the scores. In general, the doses were slightly larger for lead than for iron; the ratio of radiation yield for electrons between lead and iron is 1.3 at 100 MeV [2]. Moreover, the distribution in Fig. 2 was almost the same as that for a tungsten target struck by 200-MeV electrons [5].

Figure 4 shows the neutron doses as a function of the angle for lead and iron targets. The effective doses were two times larger for lead than for iron; the ratio of photoneutron yield between lead and iron has been reported to be 2.8 at 100 MeV [2]. The curves became gentle, peaking around 90°, which may be due to the target shape. The magnitudes increased with the electron energy; in particular, at 30 MeV, the doses were clearly smaller. The doses were considerably smaller than the photon doses in Figs. 2 and 3. At 150°, however, the neutron doses were as much as half of the photon doses. All the neutron doses were less than $20 \text{ Sv hr}^{-1} \text{ m}^2 \text{ kW}^{-1}$ [2].

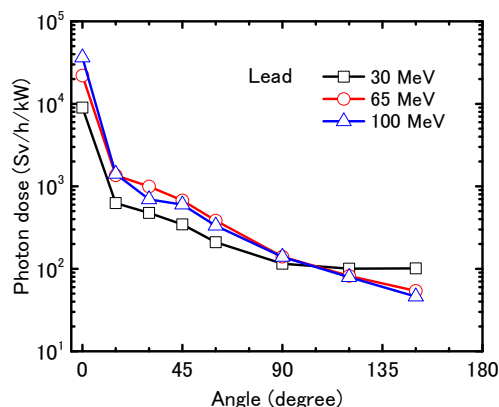


Figure 2: Photon dose rates at 1 m from lead struck by 30-, 65- and 100-MeV electrons as a function of emission angle.

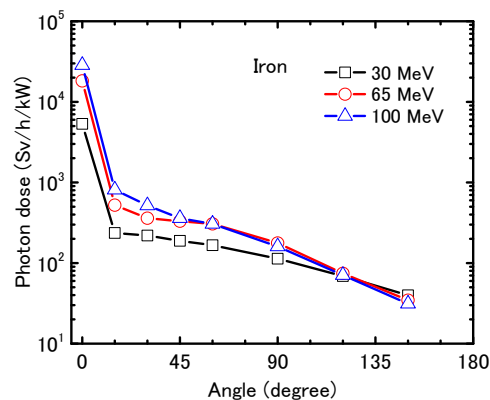


Figure 3: Photon dose rates at 1 m from iron struck by 30-, 65- and 100-MeV electrons as a function of emission angle.

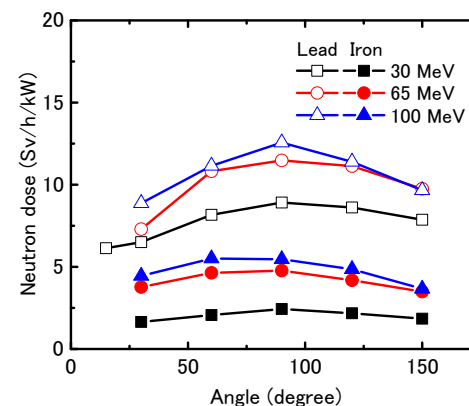


Figure 4: Neutron dose rates at 1 m from lead and iron struck by 30-, 65- and 100-MeV electrons as a function of emission angle.

Figure 5 shows the isodose contours at the side of the chicane. The dose peak appeared between 100 and 150 cm on the X axis, and the magnitude was 0.56 mSv for three months with an error of 30%, which was converted using the permitted electron number of the test linac for three months of 4.32×10^{16} . However, the dose calculated using an analytical expression [6] was 0.83 mSv. Both values were below the dose limit during the period in the uncontrolled area of 1.3 mSv.

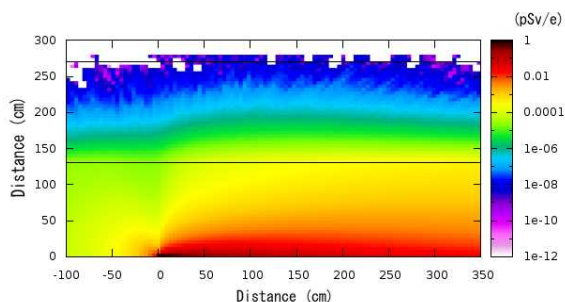


Figure 5: Photon isodose near the S3 loss point at 100 MeV, which is situated at the origin. The beamline is situated on the X axis. The concrete wall is located between $Y = 130$ cm and 270 cm.

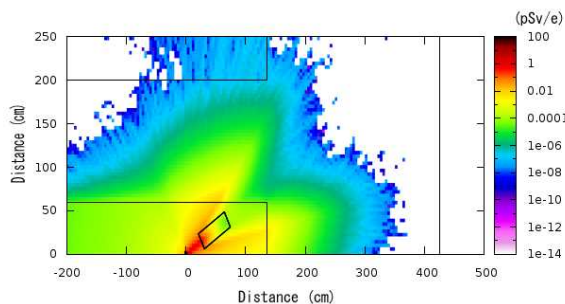


Figure 6: Photon isodose near the S5 loss point without the local shield. The slit is situated at the origin in the direction of 30° with respect to the X-axis.

Figure 6 indicates the isodose contours at the side of the S5 slit without the local lead shield. The maximum dose outside the shield was observed around $X = 110$ cm, as shown in Fig. 7, which is situated near the corner and 30° from the slit. The value was 6.9 mSv for three months with an error of 12%. The dose was 5.3 times larger than the limit. The doses when the local shield was set as in the facility are shown in Fig. 8. The doses were suppressed lower than the limit. As expected from the figure, the distribution depends on the position of the local shield; the photons leak through the gap with the dump. The doses with and without the local shield deduced from the

expression in [6] were 0.39 mSv and 6.1 mSv for three months, respectively.

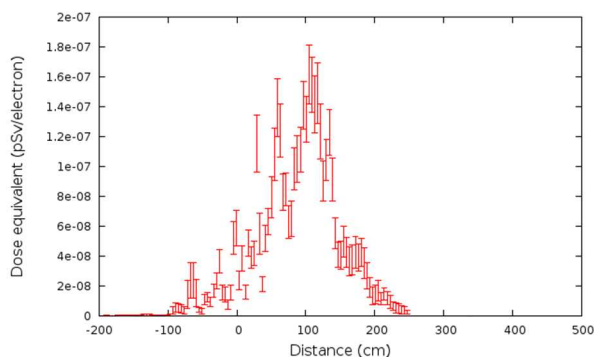


Figure 7: Photon dose distribution of Fig. 6 outside the side wall with error bars of 1σ .

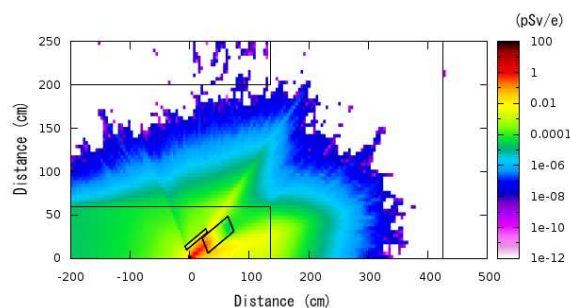


Figure 8: Photon isodose near the S5 loss point with the 5-cm-thick local shield made of lead set by the slit.

CONCLUSION

In the calculations of angular distribution, the validities of the code and input were confirmed by comparison with the reported results. The shielding calculations using the code demonstrated that the doses were smaller than the limit in agreement with those predicted with the analytical expression. Because the S5 slit was closer to the back concrete wall owing to the modification, it became easier to suppress the dose at the side wall by the local shield.

REFERENCES

- [1] T. Taniuchi, et al., "Upgrade of a photocathode RF gun at SPring-8", Proceedings of the 2004 FEL Conference, Trieste, 431-434.
- [2] W.P. Swanson, "Radiological safety aspects of the operation of electron linear accelerators", IAEA Technical Reports Series No. 188 (1979).
- [3] A. Ferrari, et al., "FLUKA: a multi-particle transport code", CERN-2005-10 (2005), INFN/TC_05/11, SLAC-R-773.

- [4] X.S. Mao, et al., “90° bremsstrahlung source term produced in thick targets by 50 MeV to 10 GeV electrons”, SLAC-PUB-7722 (2000).
- [5] A. Fasso, et al., “Radiation problems in the design of the large electron-positron collider (LEP)”, CERN 84-02 (1984).
- [6] T.M. Jenkins, “Neutron and photon measurements through concrete from a 15 GeV electron beam on a target – comparison with models and calculations”, Nucl. Instru. Meth. 159, 265-288 (1979).